

Vibrational Behaviour of Composite Beams Based on Fiber Orientation with Piezo Electric Patches

Palani Krishna Satya Mallik¹, Dr. D. Srinivasa Rao²

¹Post Graduate Student, Department Of Mechanical Engineering(M.Tech Machine Design), DMSSVH College Of Engineering, Machilipatnam, India

²Professor, Department Of Mechanical Engineering, DMSSVH College Of Engineering, Machilipatnam, India

ABSTRACT: A smart structure can sense the vibration and generate a controlled actuation, so that the vibration can be minimized. For this purpose, smart materials are used as actuators and sensors. Among all the smart materials Lead Zirconate Titanate (PZT) is used as smart material and the smart structures are taken as carbon-epoxy cantilever beams. In the present work an attempt has been made to study the effect of dimensions of PZT and position of PZT on the natural frequency of smart structure. In this work the simulation analysis and experimental analysis were carried out on the carbon epoxy cantilever beams for different fibre orientations like 0° , 30° and 60° with and without PZT patch at different positions. The simulation is carried out by using ANSYS and experimentation is carried out by using FFT analyser, accelerometer and impact hammer. Both the experimentation and simulation results show the effective control in the vibration of the structure, the required decrease in the natural frequency is observed with reference to the both patch dimension and position. Thus the results of this work conclude that the dimensions of the PZT and positioning of the PZT influences the natural frequency of the smart structure.

Keywords: Ansys, FFT Analyser, Modal Analysis, Natural frequency, Piezoelectric Material.

I. INTRODUCTION

Vibration is the motion of a particle or a body or system of related bodies displaced from the position of equilibrium. When the body displaces they occurs a loss of energy to the environments. When the body displaces to higher altitudes then it exhibits maximum potential energy and when it reaches to lowest position then it exhibits maximum kinetic energy. This tells the translation of kinetic energy to potential energy and from potential energy to kinetic energy, when the body moves between two exciting positions about a mean or equilibrium position. This is because of the elastic forces existing in the structural members.

Smartness defines self-adaptability, self-sensing, memory and multiple functionalities of the materials or structures. These characteristics provide several possible applications for these materials and structures in aerospace, manufacturing, civil infrastructure systems, biomechanics and environment. Self-adaptation characteristics of smart structures are a great benefit that utilizes the embedded variation of smart materials like shape memory alloys. By changing the properties of smart materials it can sense faults and cracks and therefore are useful as an analytical tool. This characteristic can be utilized to activate the smart material embedded in the host material in a proper way to compensate for the fault. This process is called as self-repairing effect.

Based on the direct and reverse effects, a piezoelectric material can act as a transducer to change mechanical to electrical or electrical to mechanical energy. When piezoelectric transducer changes the electrical energy to mechanical energy it is called as piezo-motor/actuator, and when it changes the mechanical energy to electrical energy it is called as Piezo-generator/sensor. The sensing and the actuation capabilities of the piezoelectric materials depend generally on the coupling coefficient, the direction of the polarization, and on the charge coefficients.

There have been many researches using finite element method to analyse piezoelectric structures. Allik and Hughes [1] applied the finite element method to analyse the three-dimensional piezoelectric vibration modes. The finite element formulation included the piezoelectric and electro elastic effect. A tetrahedral finite element was also presented based on the threedimensional electro-elasticity. Kunkel, H. A., Locke, S., Pikeroen, B. [2] applied the finite element method to calculate the natural vibration modes of the piezoelectric ceramic disks. To optimize the disk geometry, the dependence of the vibration mode on the disk diameter-to-thickness ratio was studied. Boucher et al. [3] developed a perturbation method to numerically determine the Eigen modes of vibration for piezoelectric transducers. The three-dimensional finite element method was formulated to pre-

dict the piezoelectric transducer resonance and anti-resonance frequencies as well as sound radiation for different sizes of the PZT cubes. Ha et al. [4] modelled laminated composite structures containing distributed piezoelectric ceramic sensors and actuators by finite element analysis. The computer code was developed to analyse the mechanical-electrical response of the piezoelectric ceramic laminated composites. Experiments were also conducted to verify the computer simulations. The comparisons between predicted and experimental results agreed well. There were also many researches via Finite element analysis about piezoelectric ultrasonic transducers and piezoelectric transformers such as Kagawa and Yamabuchi [5], Challande [6] and Tsuchiya and Kagawa [7]. Wang [8] generalized the formulation of frequency response functions (FRFs) for continuous structure systems subject to various forms of actuators and sensors. The actuator and sensor Eigen functions (mode shapes) were respectively identified and physically interpreted according to the testing procedures, either roving the actuator or the sensor. Wang's work provided with the theoretical base for the application of smart materials, such as PZT actuators and PVDF sensors, to smart structural testing.

In this paper, the calculation of natural frequencies of carbon epoxy composite beams having different layer orientations like 0°, 30° and 60° with bonded PZT patches have been calculated both by simulation and experimentation. For simulation the finite element method software package ANSYS 16.2 was used. The experiment is carried out on carbon epoxy composite beam having PZT patches using FFT analyser working on DEWESOF software. The process is repeated for different dimensions of PZT patches at different positions along the length of the beam.

II. THEORETICAL FORMULATION

The constitutive equation of a linear piezoelectric material is

$$\{T\} = [C^E] \{S\} - [e] \{E\} \quad \dots\dots\dots(1)$$

$$\{D\} = [e] \{S\} + [\epsilon^S] \{E\} \quad \dots\dots\dots(2)$$

Or equivalently $\begin{Bmatrix} \{T\} \\ \{D\} \end{Bmatrix} = \begin{bmatrix} [C^E] & [e] \\ [e]^T & -[\epsilon^S] \end{bmatrix} \begin{Bmatrix} \{S\} \\ \{E\} \end{Bmatrix} \dots\dots\dots(3)$ Where,

$\{T\} = \{ T_{11} T_{22} T_{33} T_{23} T_{13} T_{12} \}^T$ is the Stress vector, $\{D\} = \{ D_1 D_2 D_3 \}$ is the Electric flux density vector, $\{S\} = \{ S_{11} S_{22} S_{33} 2S_{23} 2S_{13} 2S_{12} \}$ is the Elastic strain vector, $\{E\} =$ Elastic field intensity vector, $[C^E] =$ Elasticity matrix, $[e] =$ Piezoelectric stress matrix and $[\epsilon^S] =$ Dielectric matrix.

The "equation 1" and "equation 2" are the usual constitutive equations for structural and electrical fields respectively, except for the coupling terms involving the piezoelectric matrix $[e]$. The elastic matrix $[C]$ is usual $[D]$ matrix represented in structural fundamentals. it can also be input directly in inverted form $[C]$ or in inverted form $[C]^{-1}$ as a general anisotropic symmetric matrix.

$$[C] = \begin{bmatrix} C_{11} & C_{12} & C_{13} & C_{14} & C_{15} & C_{16} \\ C_{21} & C_{22} & C_{23} & C_{24} & C_{25} & C_{26} \\ C_{31} & C_{32} & C_{33} & C_{34} & C_{35} & C_{36} \\ C_{41} & C_{42} & C_{43} & C_{44} & C_{45} & C_{46} \\ C_{51} & C_{52} & C_{53} & C_{54} & C_{55} & C_{56} \\ C_{61} & C_{62} & C_{63} & C_{64} & C_{65} & C_{66} \end{bmatrix} \dots\dots\dots(4)$$

The piezoelectric stress matrix $[e]$ relates the electric field vector $\{E\}$ in the order X,Y,Z to the stress vector $\{T\}$ in the order X,Y,Z,XY,YZ,XZ and is of the form:

$$[e] = \begin{bmatrix} e_{11} & e_{12} & e_{13} \\ e_{21} & e_{23} & e_{23} \\ e_{31} & e_{32} & e_{33} \\ e_{41} & e_{42} & e_{43} \\ e_{51} & e_{52} & e_{53} \\ e_{61} & e_{62} & e_{63} \end{bmatrix} \dots\dots\dots(5)$$

The piezoelectric matrix can also be input as a piezoelectric strain matrix $[d]$. ANSYS will automatically changes the piezoelectric strain matrix $[d]$ to a piezoelectric stress matrix $[e]$ using the elasticity matrix $[c]$ at the first defined temperature.

$$[e] = [c] [d] \dots\dots\dots(6)$$

The orthotropic dielectric matrix $[\epsilon^S]$ uses the electrical permittivity's and is of the form.

$$[\epsilon^S] = \begin{bmatrix} \epsilon_{11} & 0 & 0 \\ 0 & \epsilon_{22} & 0 \\ 0 & 0 & \epsilon_{33} \end{bmatrix} \dots\dots\dots(7)$$

The anisotropic dielectric matrix at constant strain $[\epsilon^S]$ is used by PLANE 223, SOLID 226 and SOLID 227 and is of the form:

$$[\epsilon^S] = \begin{bmatrix} \epsilon_{11} & \epsilon_{11} & \epsilon_{11} \\ \epsilon_{11} & \epsilon_{22} & \epsilon_{11} \\ \epsilon_{11} & \epsilon_{11} & \epsilon_{33} \end{bmatrix} \dots\dots\dots(8)$$

The dielectric matrix can also be inputs as a dielectric permittivity matrix at constant stress $[\epsilon^T]$ the program will automatically change the dielectric matrix at constant stress to a dielectric matrix at constant strain.

$$[\epsilon^S]^T = [\epsilon^T] - [e]^T [d] \dots\dots\dots(9)$$

Where, $[\epsilon^S]$ = Dielectric permittivity matrix at constant strain, $[\epsilon^T]$ = Dielectric permittivity matrix at constant stress, $[e]$ = Piezoelectric stress matrix and $[d]$ = Piezoelectric strain matrix.

III. FINITE ELEMENT ANALYSIS

The Cantilever beam was developed in ANSYS 16.2 is used to determine natural frequencies which are the essential parameters in design of a structure for dynamic load conditions. The beam chosen initially is a carbon epoxy composite beam of rectangular cross section for the purpose of analysis. The simulation is carried out indifferent fiber orientation like 0^0 , 30^0 and 60^0 . In this analysis mainly three conditions are considered first one is fiber orientation, the second one is varying the dimensions of PZT patch and third one is patch position. The properties of the composite beam and PZT material are shown from table 1 to 5.

Table 1: Orthotropic Properties of the Carbon-Epoxy Composite Material

Young's modulus (E_x)	$126 \times 10^9 \text{ N/m}^2$
Young's modulus (E_y)	$9.5 \times 10^9 \text{ N/m}^2$
Young's modulus (E_z)	$9.5 \times 10^9 \text{ N/m}^2$
Poisson's ratio (ν_{xy})	0.263
Poisson's ratio (ν_{yz})	0.263
Poisson's ratio (ν_{xz})	0.27
Shear modulus (G_{xy})	$1.07 \times 10^9 \text{ N/m}^2$
Shear modulus (G_{yz})	$0.8063 \times 10^9 \text{ N/m}^2$
Shear modulus (G_{xz})	$1.07 \times 10^9 \text{ N/m}^2$
Density (ρ)	1600 kg/m^3

Table 2: Anisotropic Properties of Piezoelectric Material

Linear Elastic anisotropic properties	
D_{11}	$1.26 \times 10^{11} \text{ N/m}^2$
D_{12}	$8.41 \times 10^{10} \text{ N/m}^2$
D_{13}	$7.95 \times 10^{10} \text{ N/m}^2$
D_{22}	$1.17 \times 10^{11} \text{ N/m}^2$
D_{23}	$8.41 \times 10^{10} \text{ N/m}^2$
D_{33}	$1.2 \times 10^{11} \text{ N/m}^2$
D_{44}	$2.3 \times 10^{10} \text{ N/m}^2$
D_{55}	$2.3 \times 10^{10} \text{ N/m}^2$
D_{66}	$2.35 \times 10^{10} \text{ N/m}^2$

Table 3: Piezoelectric Properties

Piezoelectric Constant Stress Matrix	
e_{12}	-5.4 C/m^2
e_{22}	15.8 C/m^2
e_{32}	-5.4 C/m^2
e_{41}	12.3 C/m^2
e_{53}	12.3 C/m^2

Table 4: Electromagnetic Properties

Electromagnetic Relativity Permittivity	
ϵ_{11}	1.151×10^{-3} F/m
ϵ_{22}	1.043×10^{-3} F/m
ϵ_{33}	1.151×10^{-3} F/m

Table 5: Density of Piezoelectric Material

Density (ρ)	7800 kg/m ³
--------------------	------------------------

The dimensions of the carbon epoxy composite beam are 0.3m x 0.03m x 0.003m. The dimensions of two PZT patch are used 0.025m x 0.015m x 0.001 m and 0.025m x 0.03m x 0.001 m.

3.1 Simulation Procedure

The composite beam is modelled by using SOLSH190 element and the piezoelectric patch is modelled by using SOLID226 element. SOLSH190 element is used to generate composite beam and layer thickness, material and orientation of fiber were specified. The beam is developed by using volume option and then enter the dimensions of the beam. For meshing purpose mesh the composite beam and PZT patch are separately by selecting the material and element type. The boundary conditions were applied to fix one end of the beam to make it as cantilever. Modal analysis is performed by using Block Lanczos method and the required first four natural frequencies were obtained from the general post processor tool bar. The same procedure was repeated to obtain the frequencies by changing the orientation of fiber like 30°, 60° of the composite beam.

Finally the same procedure was repeated for the composite beams with PZT patch, by adding the selection of volume option in the initial stage. Then enter the dimensions of the PZT patch and patch positioning. The PZT patches are placed at different positions like $L_1=0.065$ m, $L_2=0.17$ m and $L_3=0.275$ of the composite beam.

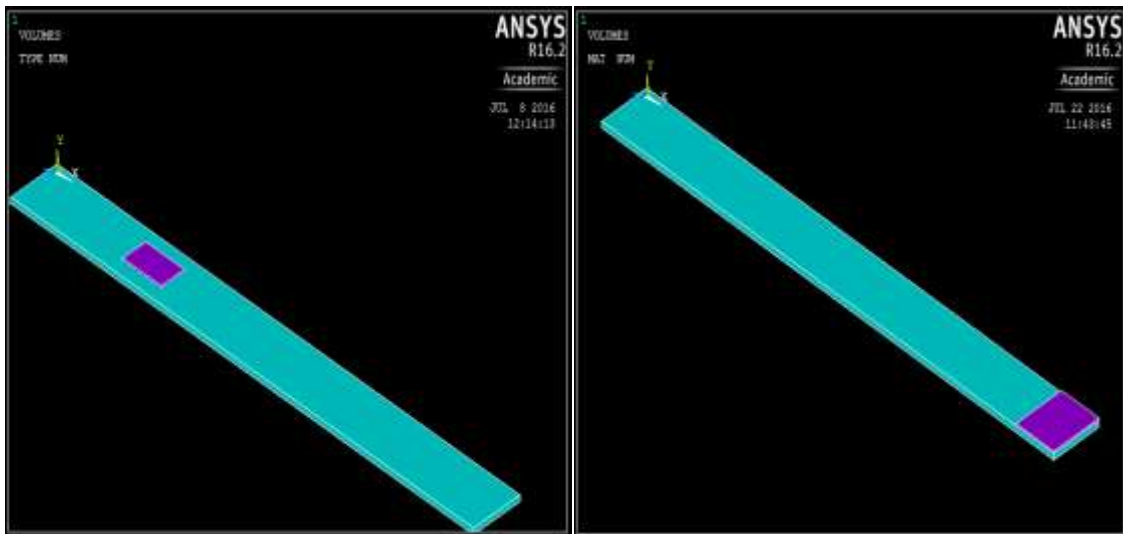


Figure 1: Composite beam with PZT patch at a Position of $L_1=0.065$ m **Figure 2:** Composite beam with PZT patch at a Position $L_3=0.17$ m when patch dimensions are Changed

IV. EXPERIMENTATION

4.1 Manufacturing Process

Composite materials are fabricated mainly in four processes they are hand lay-up, spray-up, vacuum bagging and automated tape. In this work Carbon epoxy composite beam was fabricated by using hand lay-up method. Hand lay-up process is used for the production of parts of any dimensions such as technical parts with a surface area of a few square feet, because of simplest composite manufacturing process, low cost tooling and good surface finish. In this fabrication process carbon fiber, epoxy (GY-257) and hardener (HY-140) were chosen to manufacture the composite beam. Now the weight of the carbon fiber were measured, experimentally 180 gm.

of epoxy was taken and the weight of the fiber taken was 50% of epoxy and the weight of the hardener taken was 30% that of epoxy.

The hardener was mixed with epoxy and stirred with epoxy continuously and applied on smooth surface of polishing cover with the help of brush. The carbon fibers are placed in 0° orientation again the above mixture is applied with the help of brush to obtain a thickness of 0.003m in total. Some weight is placed on the top of the system.



Figure 3: Carbon fiber



Figure 4: Epoxy



Figure 5: Squeegee of Carbon Epoxy composite



Figure 6: Carbon Epoxy composite plate

The Entrapped air is removed manually with the help of squeegees to complete the composite structure. A squeegee is a tool which is used to remove the air bubbles and surface finishing on the composite material. Now dry the composite material for 24 hours, later it was cut in to our required dimensions.



Figure 7: Carbon epoxy composite beams in fiber orientation 0° , 30° and 60°

4.2 Experimentation Procedure

The carbon epoxy cantilever beam is fixed at one end on the table by using c- clamped fixture and other end is hanging freely hence it is a cantilever beam. The accelerometer is placed on the composite beam with the help of the wax and the accelerometer and impact hammer is connected to the data acquisition system (DAQ). The DAQ is the process of measuring physical phenomenon such as vibration with the help of computer. A DAQ system consists of sensors, DAQ measurement hardware and a computer with programmable software like DEWESOFT. Now open the DEWESOFT software then enter the sensitive values of the accelerometer and hammer. Next go to measure option click on FFT graph and hammer graph and then click on store option. Next hit on the composite beam with the help of impact hammer which is connected to the DAQ system. Next go to the analysis option click on over view then check the results.

The same procedure is repeated for the composite beams with different fiber orientation and PZT patches are placed at different positions $L_1=0.065\text{m}$, $L_2=0.17\text{m}$ and $L_3=0.275$ of the composite beam



Figure 8: Experimental set up

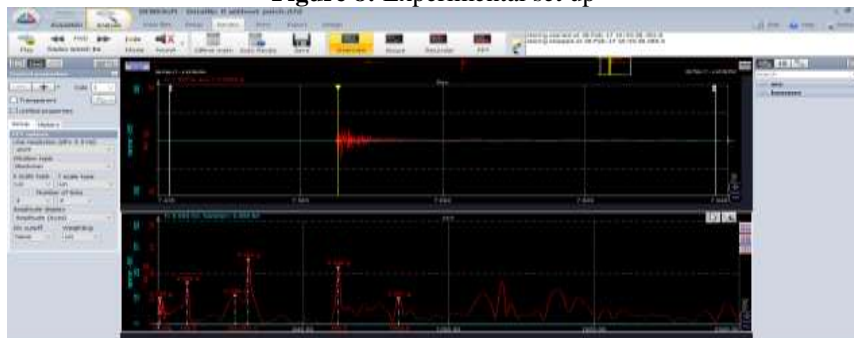


Figure 9: Schematic diagram of DEWESOFT

V. RESULTS

Simulation is done using ANSYS16.2 and experimentation is done using FFT analyser on the composite beam at 0° fiber orientation and then calculation of the first four Natural frequencies of the beams is carried out. Later the analysis is continued by changing the fiber orientations like 30° and 60° . In the next step analysis is carried out by placing PZT patch at $L_1=0.065\text{m}$. Later analysis is continued at different positions of the PZT patch $L_2=0.17\text{m}$ and $L_3=0.275\text{m}$ from the fixed end of the composite beam. In the next step the analysis is continued on the composite beam, when PZT patch dimensions are changed.

The “Fig 10” and “Fig 11” shows that when the orientation of the fibres is changed from 0° to 30° and 60° it is observed that the natural frequency is decreases with increase in the orientation of the fibres. When the fibres are lying along the length of the beam they support maximum share load on the beam, then the strength of the beam increases. After PZT patch is placed at different positions $L_1=0.065\text{m}$, $L_2=0.17\text{m}$ and $L_3=0.275\text{m}$ it is observe that when the PZT patch is placed at $L_3=0.275\text{m}$ of the beam more vibration is controlled shown in the “Fig 14” compared to the positions $L_1=0.065\text{m}$ and $L_2=0.17\text{m}$ shown in the “Fig 12” and “Fig 13”. The patch dimensions are also influences the vibration on the composite beam shown in the “Fig 14”. Therefore it can be concluded that the natural frequencies of a composite beam is decreased depends on the PZT patch positioning and patch dimensions.

5.1 Composite beams at different fiber orientation without PZT patch

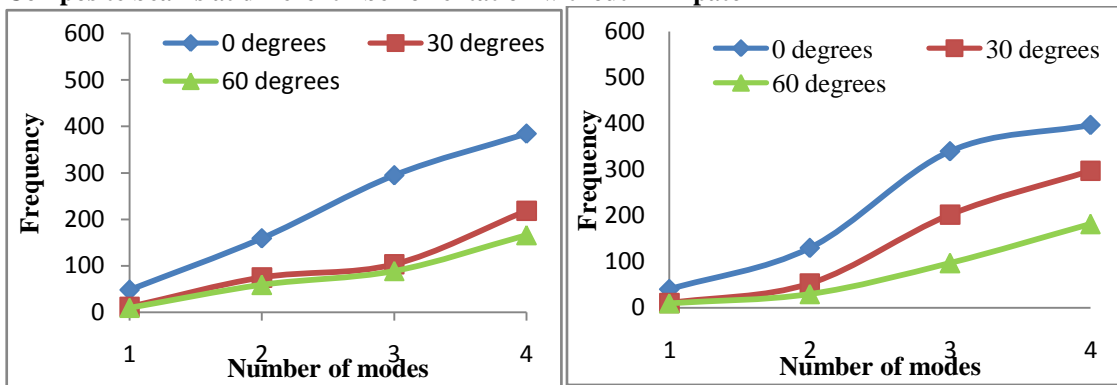


Figure 10: Simulation comparisons of composite Beams
Figure 11: Experimental comparisons of composite Beams

5.2 Composite beam with 0° fiber orientation with PZT patches

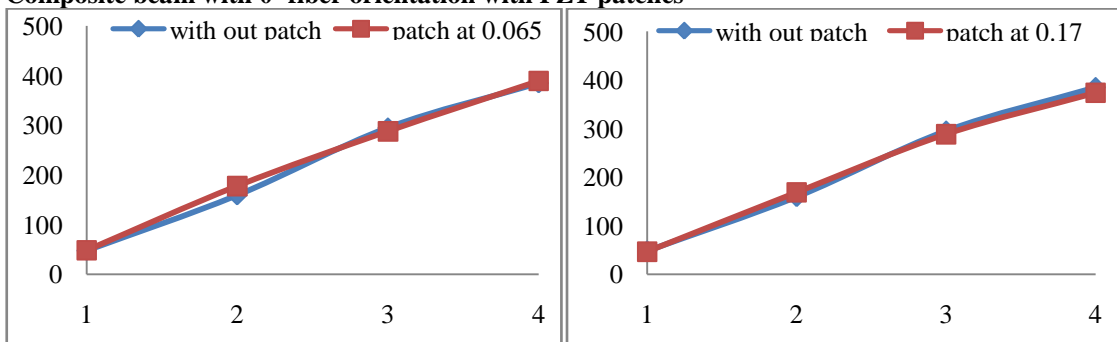


Figure 12: Mode v/s Frequency at position $L_1=0.065m$
Figure 13: Mode v/s Frequency at position $L_2=0.17m$

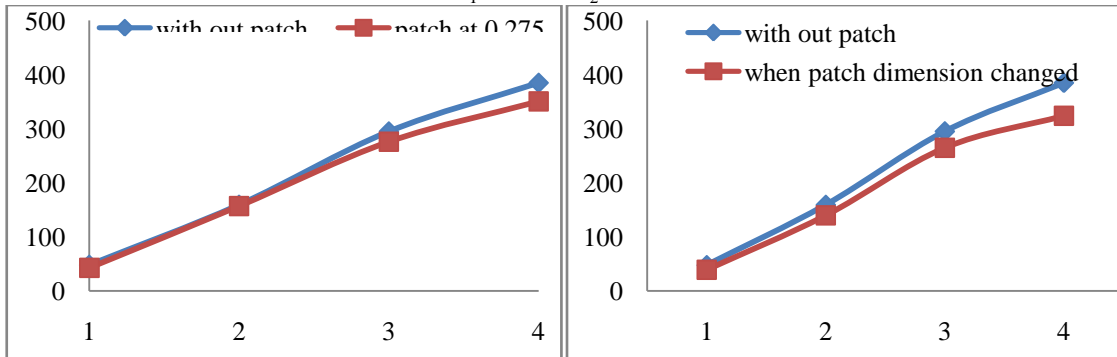


Figure 14: Mode v/s Frequency at position $L_3=0.275m$
Figure 15: Mode v/s Frequency when patch dimensions changed at position $L_3=0.275m$

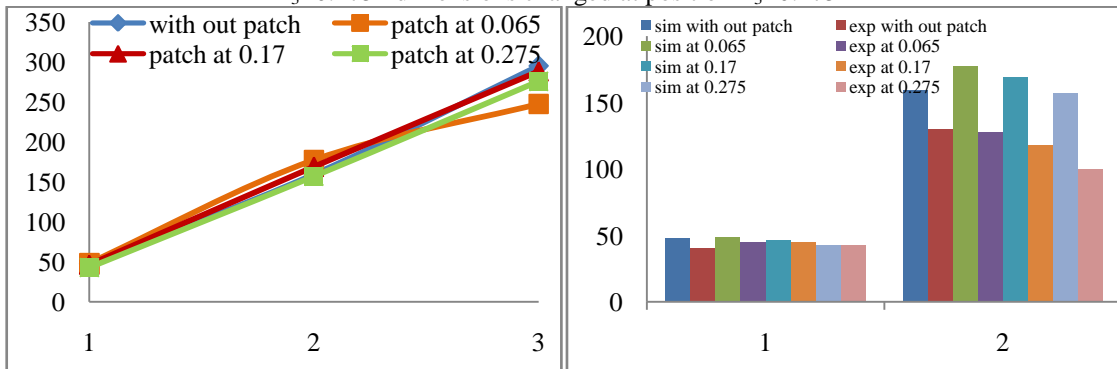


Figure 16: Simulation comparison of Mode v/s Frequency at with position L_1, L_2 and L_3
Figure 17: Simulation and Experimental comparison Mode v/s Frequency at position L_1, L_2 and L_3

5.3 Composite beam with 30° fiber orientation with patches

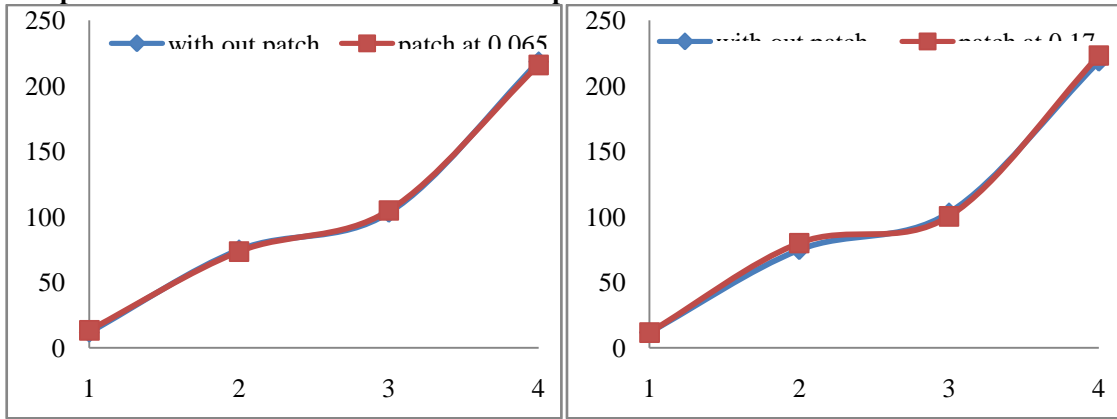


Figure 18: Mode v/s Frequency at position $L_1=0.065m$ Figure 19: Mode v/s Frequency at position $L_2=0.17m$

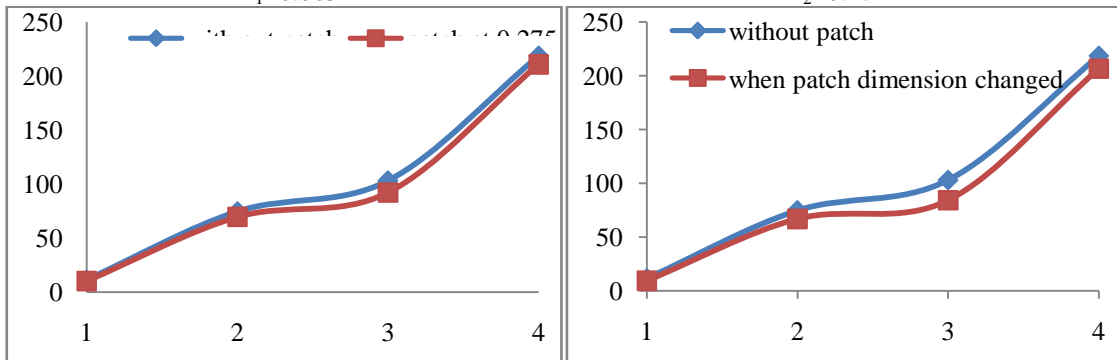


Figure 20: Mode v/s Frequency at position $L_3=0.275m$ dimensions changed at position $L_3=0.275m$ Figure 21: Mode v/s Frequency when patch dimensions changed at position $L_3=0.275m$

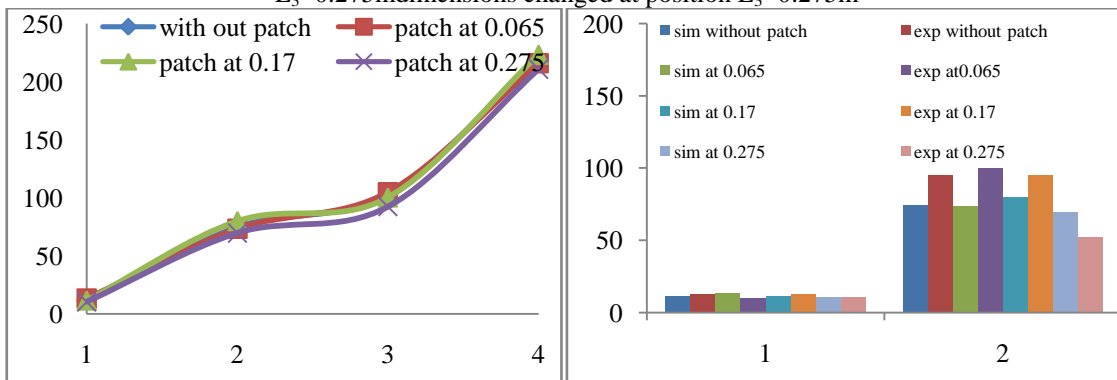


Figure 22: Simulation comparison of Mode v/s Frequency at with position L_1, L_2 and L_3 Figure 23: Simulation and Experimental comparison Mode v/s Frequency at position L_1, L_2 and L_3

5.4 Composite beam with 60° fiber orientations with PZT patches

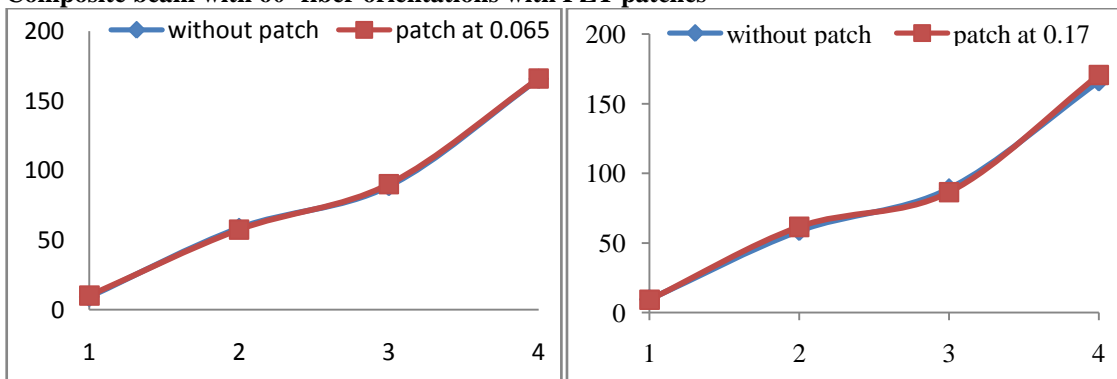


Figure 24: Mode v/s Frequency at position $L_1=0.065m$ Figure 25: Mode v/s Frequency at position $L_2=0.17m$

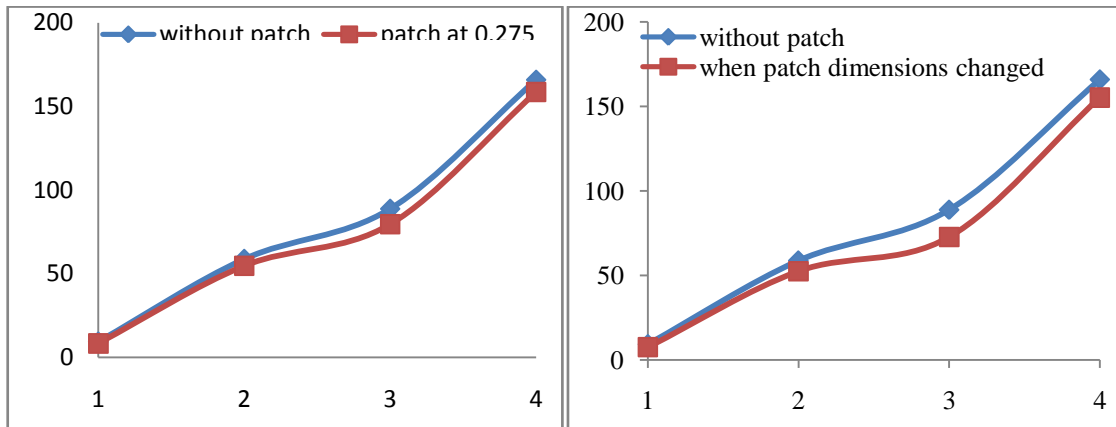


Figure 26: Mode v/s Frequency at position $L_3=0.275m$ dimensions changed at position $L_3=0.275m$ Figure 27: Mode v/s Frequency when patch dimensions changed

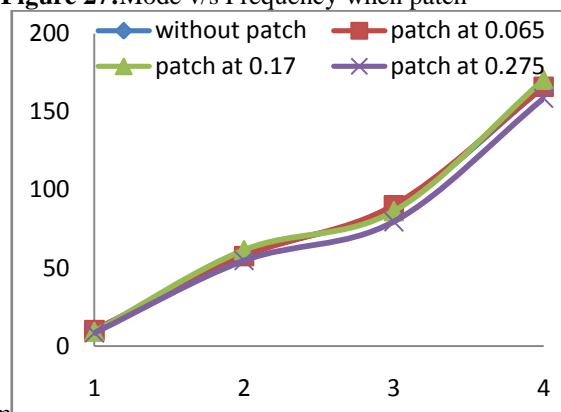


Figure 28: Simulation comparison of Mode v/s Frequency at with position L_1 , L_2 and L_3

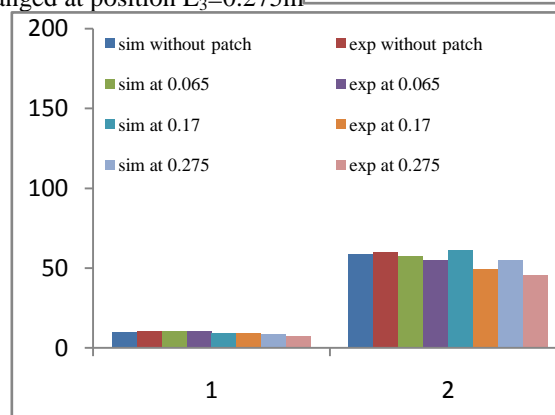


Figure 29: Simulation and Experimental comparison Mode v/s Frequency at position L_1 , L_2 and L_3

VI. CONCLUSIONS

In this present work the carbon epoxy composite beam of dimensions $0.3m \times 0.03m \times 0.003m$ were simulated in ANSYS and fabricated for experimentation keeping the orientation of fiber as 0° , 30° and 60° . The first four natural frequencies were found for all these beams with and without presence of PZT patches having different dimensions embedded to the beam at different positions. It is observed, as the size patch increases at end position of the beam, the first four natural frequencies decreases. Similarly as position of patch at same dimension changes from fixed end to free end of the beam, the natural frequencies decreases, hence the both size of the patch and position of it along length of the beam are influences the natural frequency. Using Mat-lab also the work can be carried out by simulating the conditions.

REFERENCES

- [1]. Allik, H., Hughes, T. J. R., "Finite Element Method for Piezoelectric Vibration", International Journal for Numerical Methods in Engineering, 2, pp. 151-157, 1970.
- [2]. Kunkel, H. A., Locke, S., Pikeroen, B., "Finite-Element Analysis of Vibrational Modes in Piezoelectric Ceramic Disks", IEEE Transactions on Ultrasonics, Ferroelectrics, and Frequency Control, 37(4), pp.316-328, 1990.

- [3]. Boucher, D., Lagier, M., Maerfeld, C., "Computation of the Vibrational Modes for Piezoelectric Array Transducers Using a Mixed Finite Element Perturbation Method", IEEE Transactions on Sonics and Ultrasonics, Su-28(5), pp. 318-330, 1981.
- [4]. Ha, S. K., Keilers, C., Chang, F. K., "Finite Element Analysis of Composite Structures Containing Distributed Piezo ceramic Sensors and Actuators", AIAA Journal, 30(3), pp. 772-780, 1992.
- [5]. Kagawa, Y., Yamabuchi, T., "Finite Element Simulation of a Composite Piezoelectric Ultrasonic Transducer", IEEE Transactions on Sonics and Ultrasonics, Su-26(2), pp. 81-88, 1979.
- [6]. Challande, C., "Optimizing Ultrasonic Transducers Based on Piezoelectric Composites Using a Finite-Element Method", IEEE Transducers on Ultrasonics, Ferroelectrics, and Frequency Control, 37(2), pp. 135-140, 1990.
- [7]. Tsuchiya, T., Kagawa, Y., "Finite Element Simulation of Piezoelectric Transducers", IEEE Transducers on Ultrasonics, Ferroelectrics, and Frequency Control, 48(4), pp. 872-878 2001.
- [8]. Wang, B. T., "Structural Modal Testing with Various Actuators and Sensors", Mechanical System and Signal Processing, 12(5), pp. 627-639, 1998.
- [9]. ANAYS 16.2 student edition.